THE CRYSTAL STRUCTURE OF TIPULA IRIDESCENT VIRUS AS DETERMINED BY BRAGG REFLECTION OF VISIBLE LIGHT

A. KLUG, ROSALIND E. FRANKLIN* AND S. P. F. HUMPHREYS-OWEN
Crystallography Laboratory and Physics Department, Birkbeck College, London (Great Britain)

(Received June 20th, 1958)

SUMMARY

Crystals of Tipula iridescent virus (TIV)[3] diffract light just as ordinary crystals diffract X-rays, so that a crystallographic study is possible using visible light.

The conditions of growth of TIV crystals have been investigated and a method developed for preparing large crystals from the microcrystalline centrifuged virus pellets. Optical observations using monochromatic light have been made on crystals oriented parallel to the face of a perspex cell. The virus concentration in the normal wet crystals is calculated from the measured refractive index to be $17 \pm 4\%$ w/v. The virus particles are packed in a face-centred cubic array, with an interparticle spacing of 2500 ± 30 Å, a distance nearly twice the diameter of the frozen-dried particle.

The nature of the crystals is discussed and it is concluded that the (hydrated) virus particles in the crystal are not in contact but are separated by large distances of water ($\sim$ 500 Å). The crystals are thus probably held together by long-range forces operating at a distance comparable with the size of the particles themselves. The TIV crystals seem to represent the first clearly established instance of an ordering of iso-dimensional colloidal particles in three dimensions.

INTRODUCTION

A cytoplasmic virus affecting the larvae of *Tipula paludosa*, the crane fly, was discovered in 1954[1,2] by the Agricultural Research Council Virus Research Unit at Cambridge[3–5]. In 1957 WILLIAMS AND SMITH[5] established, using shadowing techniques with the electron microscope, that the particle, when frozen-dried, has the shape of a regular icosahedron and a diameter of about 1300 Å. There was apparently complete uniformity in size and shape despite the large size.

Centrifuged pellets of the purified virus are iridescent when viewed by reflected light[3]—hence the name, Tipula Iridescent Virus (TIV), given to the virus by SMITH AND WILLIAMS[4]. The pellets consist of a mass of randomly oriented crystallites in which the spacings between the virus particles are so large that they are comparable with the wavelengths in the visible spectrum. Every crystallite that lies in an appropriate orientation with respect to the incident beam of white light will reflect a particular

* Deceased 16th April, 1958.

References p. 219.

wavelength which depends on the inter-particle spacing within the crystallite. The effect is analogous to the reflection of X-rays by simple crystals, and is governed by Bragg's law, according to which the wavelength selectively reflected is proportional to the sine of the glancing angle and to the distance between successive reflecting planes in the crystal (equation (2) below).

An investigation of the TIV crystal structure by X-ray methods would not be practicable because the very large unit cell would cause X-ray reflections to be more crowded together than the limit of resolution. However, the iridescence and its interpretation[3] indicate that an investigation by methods analogous to X-ray crystallography but using visible light is possible. Such an investigation is described in this paper.

We have found that the inter-particle distance in the crystal is apparently much greater than the diameter of the particles; that is, neighbouring particles are separated from one another by a layer of water some hundreds of ångstroms thick. This means that the interparticle forces are of the same kind as those in oriented gels of tobacco mosaic virus (TMV)[25], and are different from those in most other protein and virus crystals. The TIV crystals appear to resemble the crystalline inclusion bodies of TMV found in infected leaf-hair cells[6], and the iridescent domains observed by OSTER[7] which separate from bottom layer TMV solution. The two latter forms of TMV both show Bragg reflection of visible light[6], but reflections from only one set of crystal planes have been observed. This applies also to the other observed instances of Bragg reflection in the visible spectrum, such as by gels of iron oxide[8,9], chloroplasts[10], films of latex spheres[11], solutions of polypeptides[12], and lamellar-twinned crystals of potassium chlorate[13]. Our investigation appears to be the first determination of a truly three-dimensional crystal structure by optical as distinct from X-ray diffraction.

I. PREPARATION AND PROPERTIES OF CRYSTALS

I.1. Material

Purified suspensions of TIV in water (about 1% concentration) were kindly supplied by WILLIAMS. Such suspensions are of milky appearance, being bluish-white when viewed by reflected light and dull red in transmission. On storage at 5° for periods of weeks there is a tendency for some of the virus to be irreversibly precipitated in a non-crystalline form. In the experiments described below we have used always the supernatant milky suspension.

I.2. Formation of crystals

In addition to the non-crystalline precipitate referred to above, a thin layer of crystals frequently forms slowly on the bottom of a glass vessel containing a TIV suspension. These crystals form most readily in preparations which show the smallest tendency to deposit a precipitate. They range up to a millimetre or more in diameter, and mostly appear either bright green or red when viewed at the appropriate angle in reflected light. Such crystals are, however, extremely unstable. They disappear rapidly when the supernatant suspension is disturbed, the red crystals being always the first to go. It seems that this is a case of crystallisation due to sedimentation under the influence of gravity, and that the crystals are in equilibrium with the supernatant only as long as the influence of gravity is undisturbed by other external forces. It is, of

References p. 219.

course, impossible to remove such crystals from the supernatant without destroying them.

For further study of the properties of these crystals it is clearly necessary to prepare them at a site where they can conveniently be studied. Attempts to prepare such crystals by conventional methods met with no success. For example, slow evaporation of the milky suspension in a capillary tube leads only to the formation first of a more concentrated suspension and then of a non-crystalline precipitate. Again, addition of ammonium sulphate in concentration as low as 5% of saturation causes the virus to precipitate within a few hours.

That centrifuged pellets of TIV are microcrystalline has been beautifully demonstrated by WILLIAMS AND SMITH[3]. The formation of microcrystals in the centrifugal field may be compared with the slow formation of larger crystals in the much weaker gravitational field; the crystallisation process is probably fundamentally similar.

In freshly prepared centrifuged pellets viewed in reflected white light there is a smooth gradation of colour ranging from violet at the bottom through green to red at the top. The different colours correspond to different degrees of hydration of the crystallites. There are no individual crystallites large enough to be visible in a low power microscope. It was observed, however, that if the supernatant liquid was not immediately and completely removed, crystals were formed rather rapidly *at the interface* between the pellet and the liquid. Again, these crystals were unstable and could not be removed from the centrifuge tube, but the observation suggested a new method for preparing crystals at more convenient sites.

It was found that crystals could be prepared more or less at will when an interface was formed between microcrystalline gel and either water or a milky suspension of the virus. The number and size of the crystals formed varies somewhat unpredictably, but the method almost always works to some extent. Crystals have been prepared by this method both in capillary tubes and on flat surfaces of glass, perspex or mica. The crystals are always thin, but have diameters up to about 1 mm. The nature of the process by which a microcrystalline gel recrystallizes to form macrocrystals when in contact with water or dilute virus suspension is not understood. The crystallization is not *solely* due to the existence of a sharp concentration gradient, since a milky suspension of similar concentration to that of the gel will not form crystals when in contact with water.

To obtain crystals of reasonable stability, the minimum necessary amount of water must be added to the microcrystalline gel. If too much water is added the crystals dissolve soon after they are formed. On the other hand, if no water is added, the microcrystalline gel can be stored for months without the appearance of macrocrystals.

It should perhaps be mentioned that there is a sharp distinction between a concentrated suspension of the virus and a microcrystalline gel of the same concentration. The gel is clear and is straw coloured when viewed in white light by transmission. The suspension is milky and is dull red in transmission.

For the quantitative optical measurements described below, crystals were prepared in a small rectangular perspex cell of dimensions $4 \times 2 \times 0.7$ mm. A little of a freshly centrifuged pellet of the virus was introduced, together with a small drop of the supernatant, and the top of the cell was sealed with paraffin wax. Crystals first appeared at the gel–liquid interface. Over a period of days the crystallisation slowly

References p. 219.

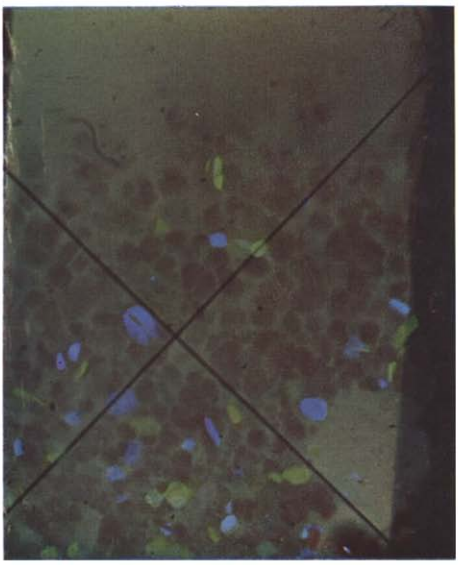

1a

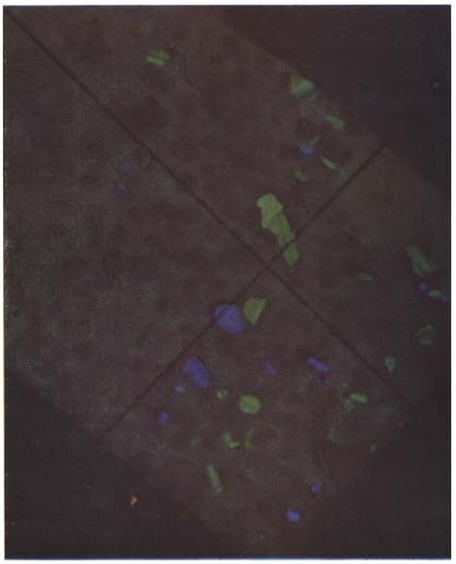

1b

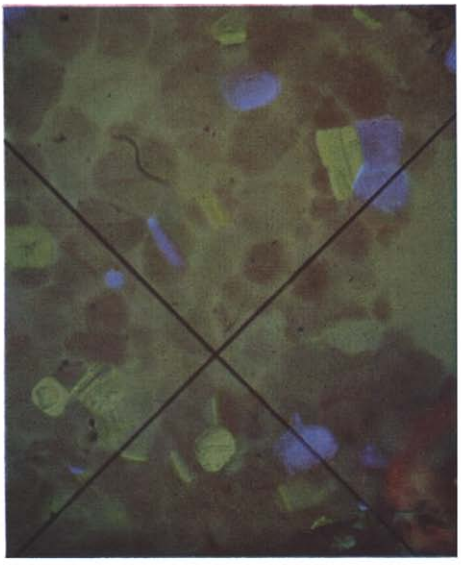

2

3

Fig. 1a. Photograph of the cell taken by back reflection in white light, when the crystals were no longer all parallel to the cell face (27 ×). Bragg reflection from the (111) planes shows up as green, and from the (200) as blue.

Fig. 1b. The same, but with the cell in a slightly different position (as shown by the position of the cross-wires) (27 ×). Different crystals are now in the correct setting to give Bragg reflections.

Fig. 2. An enlargement of a portion of Fig. 1a (58 ×). Note the occurrence of stacks of plate-shaped crystals.

Fig. 3. Photograph of the cell taken by back reflection in white light, after it has been allowed to dry out slowly (32 ×). Violet reflections only are observed from the crystals, showing that they have shrunk.

extended throughout the cell until the whole of the perspex surface was covered with crystals, which reflected green or turquoise at small angles of incidence and blue or violet at larger angles. The individual crystals were thin plates which were found to lie predominantly parallel to the cell face (see section II below). After some weeks this orientation was lost, and photographs (Fig. 1) show reflection at angles different from the angle of incidence to the cell face.

I.3. Qualitative observations on the crystals

Observations on preparations of macrocrystals indicated that the turquoise-reflecting crystals represent to some extent a preferred state. On preparing crystals as described above, a good number of red-reflecting crystals are initially visible. But these invariably disappear after a short time and before any drying out of the specimen has occurred, only the turquoise-reflecting crystals remaining. Furthermore, when a centrifuged pellet is allowed to dry, the crystals shrink, as shown by the change in reflected colour from turquoise to violet[3]. The effect is reversible[3], the colour being restored to turquoise on rehydrating a partially dried pellet.

Observations on the shrinkage of the crystals prepared in the perspex cell described above also point to the comparative stability of the turquoise crystals. The cell was not completely air-tight and the contents dried out very slowly (Fig. 3). It was clear that the shrinkage of the crystals did not keep pace with the drying out of the cell as a whole. There was a period of weeks in which the colour reflected by the crystals did not change noticeably, in spite of a large decrease in the volume of the associated milky suspension (Fig. 1).

Thus it seems that the turquoise-reflecting crystals, once formed, tend to retain the water associated with them while the concentration of virus in the surrounding solutions varies within rather wide limits.

It is often observed that the crystals formed on glass or mica as described above bear parallel bands on their surface, which are alternately bright and dark. Observations with crystals on a microscope slide show that there are two positions, symmetrical with respect to the direction of the incident light, in which alternate bands are at their brightest or darkest respectively. This suggests some kind of lamellar twinned structure, which we have, however, not investigated in detail. The bands vary a good deal in width; some rather broad bands are visible in Figs. 1 and 2, but the narrowest we have observed are only 1.5 μ wide. Many, apparently single, crystals do in fact have the form of very thin plates, and often a number of these are seen stacked one above the other (Fig. 2).

II. OPTICAL MEASUREMENTS

II.1. Quantitative optical observations

It was first established that the crystals in the cell were oriented with crystal planes parallel to the cell face. A polycrystalline, random, mass would always diffract monochromatic light at a particular angle which is independent of the orientation of the mass with respect to the incident beam, (*cf.* an X-ray powder photograph). In the case of a freshly prepared cell of TIV crystals, reflection for a given wavelength is obtained only under specular conditions (angle of incidence equal to angle of reflection) with respect to the cell face, and moreover the angle of incidence which gives reflection

References p. 219.

is a direct function of the wavelength. Finally it was confirmed that rotation of the cell in its own plane made no difference. Thus it was concluded that Bragg reflection was taking place from crystal planes themselves parallel to the cell face.

The intense continuous spectrum from a xenon gas arc was dispersed by a Hilger monochromator. The latter has a calibrated drum by which a narrow band (depending on slit widths) of wavelengths can be selected. The calibration was carefully checked. The horizontal emergent beam was rendered parallel by a lens and was incident on the perspex cell. The cell was located on the central stage of a spectrometer with its reflecting face vertical and normal to the horizontal plane containing the incident and reflected beams. The reflected beam entered the telescope of the spectrometer and was observed by eye. Independent rotation, about a vertical axis, of the stage carrying the cell and of the telescope was provided and enabled any angles of incidence or reflection with respect to the cell face to be selected and measured.

In the specular condition reflection from the perspex surface will always produce an image of the exit slit of the monochromator. But when, for a particular wavelength, the angle of incidence is also correct for Bragg reflection from the crystals, this weaker light must be distinguished from the reflection from the perspex. In practice there was no difficulty because, owing to the small thickness of the crystals examined, the Bragg reflections were spread over an appreciable angular range.

The procedure was to select an angle of incidence, establish the specular condition by rotating the telescope until the slit image was in the centre of the field of view, and then to rotate the wavelength drum of the monochromator until Bragg reflection occurred. This was recognised by the field of view suddenly appearing lit up on both sides of the slit image. By this method it was found that the wavelength giving maximum intensity of the Bragg reflected light could be determined to within about 10 Å in the green and about 20 Å in the violet. Readings obtained by three different observers agreed within this range. The results are given in Table I, in which, following usual crystallographic practice, we employ the glancing angle in place of the angle of incidence (see also Fig. 4).

TABLE I

WAVELENGTH λ AT WHICH THE INTENSITY OF THE BRAGG REFLECTION IS A MAXIMUM FOR A SETTING α

i degrees	α degrees	111 reflection $m\mu$	200 reflection $m\mu$	Ratio $\lambda_{200}/\lambda_{111}$
9	81	555	495.5	0.893
13.5	76.5	551	492.5	0.894
18.5	71.5	545	485	0.890
23.5	66.5	537	479	0.892
28.5	61.5	527	467	0.887
33.5	56.5	514	457.5	0.885
38.5	51.5	500.5		
43.5	46.5	488		
48.5	41.5	470		
53.5	36.5	454.5		
58.5	31.5	438		

For any given angular setting of the cell Bragg reflections are observed at two different wavelengths. At small angles of incidence a strong reflection occurs in the

References p. 219.

green at a wavelength of about 560 mμ, and a weaker one in the blue-violet at about 500 mμ. The ratio of the two wavelengths is constant for all angles of observation and is close to 1:0.89 (See Table I). Hence, by Bragg's law, the ratio of the corresponding crystal lattice spacings is approximately 0.89.

Now WILLIAMS AND SMITH[3] deduced from electron micrographs of sections of virus pellets that the lattice is face-centred cubic. For this lattice the two largest interplanar spacings are from the (111) and (200) planes and their ratio is 1:0.866. Our results therefore confirm their deduction. The 2.5 % discrepancy can be accounted for by dispersion. Our ratio is for vacuum wavelengths (geometrical path) whereas the true ratio should be for optical paths, *i.e.*, $(n_c d)_{111}/(n_c d)_{200}$ where n_c is the refractive index of the crystal and d is the spacing (see section II.2). For proteins[14] n is greater for violet than for blue light by about 2 or 3 %, and therefore our observed ratio agrees with a strictly face-centred cubic structure.

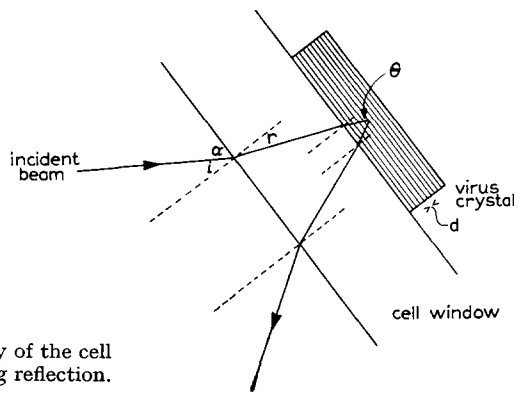

Fig. 4. Geometry of the cell and of the Bragg reflection.

It should be added that some form of packing closely approximating this cannot be entirely ruled out. In this case the true unit cell would have planes with spacings greater than that of the (111) planes of a face-centred cubic lattice, but these would give Bragg reflections for wavelengths beyond the red limit of the visible spectrum. A body-centred cubic structure is definitely ruled out since in this case the ratio of the two largest spacings would be 1:0.707. A hexagonal close-packed lattice is very similar to a face-centred cubic lattice as far as the arrangement of the 12 nearest neighbours about a central particle is concerned, and it also has crystal planes with spacings in the ratio 0.866. These are not, however, the lowest order planes and the corresponding interparticle distance would turn out to be much too large to be compatible with the concentration of virus in the crystal of TIV. Hence this lattice is also ruled out.

It might be thought that in view of the electron microscope results this additional and less direct evidence for a face-centred cubic lattice is superfluous. However, it is known that for several plant viruses high quality electron micrographs[15–17] indicate a face-centred cubic lattice whereas X-ray diffraction[18,19] from the wet crystals shows that the crystal lattice is in fact body-centred or, in the case of sourthern bean mosaic virus[20], more complicated. In these cases it must be supposed that the face-centred cubic crystals are formed during the preparation of specimens for electron microscopy. The present results show that in the case of TIV the untreated wet crystals are in fact face-centred cubic.

References p. 219.

It follows from our interpretation that the crystals tend to set themselves with either their (111) or (200) planes parallel to the cell face. This is supported by Fig. 1 in which the two cases (green and blue crystals respectively) can be seen. That we have observed only two reflections is not surprising, since no Bragg reflections from crystal planes other than (111) and (200) occur in the visible spectrum. The wavelengths necessary to observe Bragg reflection from the planes of next largest spacing, (220), are lower by a factor of $1/\sqrt{2}$ than those required for the (200) spacing, and so lie in the ultra-violet. No quantitative observations could be made with our cell and apparatus, though this would be possible if quartz cells and sufficiently powerful light sources were used. We have taken photographs of the cell in ultra-violet light of wavelength 3600 Å and Bragg reflections are clearly visible.

II.2. Analysis of the optical observations

The optical geometry is shown in Fig. 4. We list symbols as under:

i = angle of incidence onto front face of cell,
r = angle of refraction in perspex,
$\alpha = 90 - i$ = glancing angle onto front face of cell,
θ = glancing angle onto crystal planes,
n_c = refractive index of crystal,
n_p = refractive index of perspex,
λ = vacuum wavelength,
$\lambda' = \lambda/n_c$ = wavelength in crystal,
d = interplanar spacing,
N = number of cooperating planes in Bragg reflection,
$t = Nd$ = thickness of crystal.

By Snell's law:

$$\sin i = n_p \sin r = n_c \sin (90 - \theta),$$

therefore

$$\cos \alpha = n_c \cos \theta \tag{1}$$

Equation (1) holds if all interfaces are parallel and is unaffected by any thin film of water which may exist between crystal and cell.

The condition for (first order) Bragg reflection in the crystal is:

$$2dn_c \sin \theta = \lambda \tag{2}$$

where λ is the wavelength *in vacuo*. θ is not an observable, and may be eliminated by combining equations (1) and (2). We obtain

$$\left(\frac{\lambda}{2d}\right)^2 + \cos^2 \alpha = n_c^2 \tag{3}$$

If the refractive index were constant over the range of wavelength considered, we see from equation (3) that a plot of λ^2 against $\cos^2\alpha$ would give a straight line of slope $4d^2$ and an intercept of $4n_c^2d^2$ on the λ^2 axis. Hence a set of measurements of the wavelength λ for maximum reflected intensity over a range of values of α would give not only the crystal spacing d but also n_c, the index of refraction of the crystal. Knowledge of n_c is very valuable, since, if the specific refractive increment of the virus is also known, we can calculate the concentration of virus in the crystal. n_c thus

References p. 219.

plays the role that density plays in conventional X-ray crystal analysis, giving the weight of the asymmetric unit in the unit cell of the crystal.

The λ^2 *vs.* $\cos^2\alpha$ curves for the 111 and 200 reflections are shown in Fig. 5. It is seen that the exact linearity expected from (3) is not obtained. The curvature is not due to dispersion because, on the one hand, the curvature is too great to be accounted for by dispersion and, on the other hand, even if dispersion were operative, it would make the curve concave upwards. In the Appendix an explanation is given of the curvature as a second order effect arising from the small thickness of the crystals. For the present purposes we shall ignore it and treat the curves as linear.

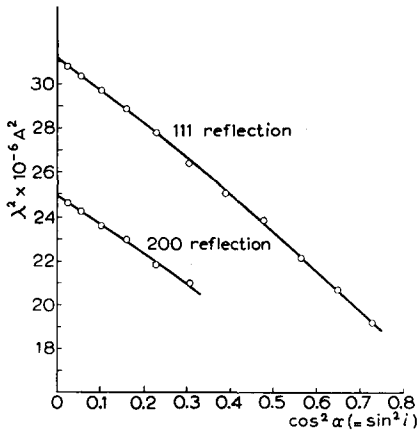

Fig. 5. Plot of λ^2 *vs.* $\cos^2\alpha$ for the 111 and 200 Bragg reflections, where λ is the wavelength *in vacuo* for which the reflected intensity is at a maximum at the setting α.

The question then arises as to how to draw the best straight line, since the curvature of the observed set of points is not due to experimental error. The theory given in the Appendix shows that the points most affected by the second-order effects are those at low values of $\cos^2\alpha$. On the other hand, the actual readings at the higher values of $\cos^2\alpha$ are the less reliable, on account of the greater difficulty of making observations in the violet than in the green. As a compromise, therefore, we have omitted the first 4 points for the 111 reflection and the first 2 for the 200 reflection. (It is not practicable to omit more points in the latter case.) From the best straight lines through the remaining points we obtain the results shown in Table II. To obtain some idea of the possible error in this procedure we have also made calculations from the best straight lines drawn through *all* points in Fig. 5. The results are given in brackets in Table II. The difference between the two sets of results is not large, being only 1.5 % in d_{111} and about 1 % in n_c. The values obtained from the 111 reflection are more reliable than those obtained from the 200 reflection, owing to the relative weakness of the latter.

Taking the unit cell side as 3580 Å, the spacing d_{110} is 2530 Å. The latter may be identified with the interparticle distance in the crystal if there is one virus particle per lattice point. That this must be the case follows from the value of n_c, which gives the concentration of virus in the crystal (see section III below), and in any case is obvious from WILLIAMS AND SMITH's electron micrographs[3] of methacrylate-embedded pellets. Thus, in the crystals as examined by us, the interparticle distance is about

References p. 219.

2500 ± 30 Å, a distance almost twice the diameter of the frozen-dried particle. The implications of this are discussed in the next section.

Repetition of the optical observations after a week showed quantitatively that there had been a 3 % shrinkage in the crystal spacings. This was produced by the slow drying out of the cell which was not completely air-tight. The subsequent shrinkage after this could not be followed, as the crystals gradually lost their orientation parallel to the cell face and our optical technique could not be used.

TABLE II

CRYSTAL SPACINGS AND REFRACTIVE INDEX

	111 reflection	*200 reflection*
$2d$	4137 Å (4070 Å)	3690 Å (3610 Å)
$2n_c d$	5635 Å (5605 Å)	5000 Å (4990 Å)
n_c	1.364 (1.377)	1.358 (1.383)
Unit cell side		
d_{100} = 3580 Å (3520 Å)	Ratio $\frac{n_c d_{200}}{n_c d_{111}}$ = 0.887	
d_{110} = 2530 Å (2480 Å)		

III. THE INTER-PARTICLE FORCES IN THE TIV CRYSTAL

III.1. Concentration of virus in the crystal

The refractive index of the crystals, found from the optical analysis (Section II) is 1.364 ± 0.008. A check on this value was made by determining the refractive index of centrifuged pellets of TIV on an Abbe refractometer. The lowest value obtained for freshly prepared pellet was about 1.365, higher values up to 1.375 being obtained when no precautions were taken to prevent the pellet from drying. Since the evidence of the electron microscope[3] indicates that the virus pellet is wholly microcrystalline, we may take these observations as confirming the above value.

The specific refractive increments of most proteins and viruses that have been investigated lie close to the value 0.00185 (for sodium light). Assuming that this value holds for TIV also, we calculate from the refractive index that the concentration of dry virus in the crystal is about 17 ± 4 % (w/v). This concentration is much lower than those usually found in crystalline proteins and crystals of the small plant viruses, which contain approximately equal amounts of dry material and of water.

However, this result is consistent with the size of the virus particle and the interparticle spacing in the crystal. Assuming that the partial specific volume of TIV lies somewhere between 0.70 and 0.74 (the respective values[22] for southern bean mosaic virus and tomato bushy stunt virus which contain a similar proportion of nucleic acid), the volume fraction occupied by the dry virus in the crystals is calculated from the concentration to be about 12 %. Taking the diameter of a dry virus particle to be 1300 Å and the interparticle spacing in the face-centred cubic lattice to be 2500 Å, the fraction of crystal volume occupied comes out to be 10.5 %.

III.2. Interparticle contact in the crystals

If icosahedra are arranged in a face-centred cubic lattice, each particle will be surrounded by 12 others, and the line connecting two neighours will pass nearly through the centres of edges. The diameter of an icosahedron in this direction has a

References p. 219.

value very close to the mean diameter of the sphere of equivalent volume. The inter-particle distance (2500 Å) is almost twice the frozen-dried diameter (1300 Å), so that the virus particles cannot touch in the crystal unless they are very heavily hydrated.

WILLIAMS AND SMITH[3] found that in electron micrographs of virus pellets or larval tissue[21] embedded in methacrylate, the virus particles nowhere appear to touch. They concluded that the virus particles were actually touching but that the outer envelope was so tenuous that it was not visible against the background. The particle does seem to possess an outer "membrane" as shown by the existence of empty shells[21], but there again there is no reason other than the apparent non-contact between neighbouring particles to believe that the membrane necessarily has a diameter greater than about 1300 Å. The results of our optical investigation on the wet crystals suggest that neighbouring particles may not in fact be in contact.

Before it can be concluded from our results that the virus particles in the crystal are not touching it is necessary to know the diameter of the particle in solution, which may be expected to be a good deal larger than the frozen-dried diameter. A wet diameter of 2500 Å, however, would mean a hydration of about 5 g water/g dry virus, which would seem a most unlikely value unless the virus particle were either an expandable bag or sponge-like. In view of both the large size and very well defined polyhedral form[5] of the virus particle, one might expect it to resemble a small protein crystal; and most protein crystals have a total hydration no larger than about 1 g water/g protein. The largest value reported for the hydration of a virus is for influenza virus which probably has a much more complicated structure than TIV since it contains lipids and polysaccharides, whereas TIV is believed to contain only protein and DNA. The reported values of the hydration in influenza virus range[22] from 0.57 to 3.78, but the upper figure is not reliable[22] since it is based on viscosity measurements. The hydration of T_2 bacteriophage, which is similar in size to both influenza virus and TIV, is only about 0.6[22].

The question of the hydrated size of the virus particle perhaps can best be settled by either small-angle X-ray or light scattering, but the reservation must be made that, as with all such methods, they would be insensitive to the existence of a tenuous outer layer*. On our own X-ray apparatus we are unable to make observations at the very low angles required for a particle of such large diameter. A study of the low angle X-ray scattering by TIV in solution has recently been made by ARNDT AND BEEMAN[23], who have very kindly communicated their preliminary results. These indicate that the hydrated diameter is about 1800 Å. This value would correspond to a hydration of 1.2 g water/g virus.

If 1800 Å is accepted as the mean diameter of the hydrated virus particle, it is most unlikely that the diameter along the direction of closest approach of two neighbouring particles would be greater than about 2000 Å. This still leaves a gap between neighbours of about 500 Å occupied presumably only by water.

III.3. Long-range forces in TIV

If the above suggestion that neighbouring particles are separated by a gap of about 500 Å is correct, it would seem that in the TIV crystal the particles are held together by the so-called long-range forces which operate over distances much larger

* WILLIAMS has examined electron micrographs of purified TIV for evidence of "whiskers" or fibrous material that might hold the particles apart, but none has been found.

References p. 219.

than the range of ordinary valency forces, and which are believed to come into play in the case of large colloidal particles[24]. Forces of this kind are operative in the case of gels of tobacco mosaic virus as is shown by the classical work of BERNAL AND FANKUCHEN[25].

Certainly, the general picture which we have formed of TIV crystals is consistent with the view that these forces are operative. The extreme fragility of the crystals would seem to indicate that the particles are not held together in the crystal in close contact. We may also cite the difficulty of growing crystals by simple concentration or precipitation: long-range crystalline order is apparently difficult to establish by these methods and requires a "seed" in the form of microcrystallites produced by centrifugation.

The fact that the interparticle distance in the crystals is variable also points to the existence of non-contact forces. It is difficult to believe that the variability in interparticle distance could be accounted for by varying degrees of hydration of particles in contact, since changes in the hydration would then have to occur in a region of low virus concentration ($\sim$ 20 %). This seems most unlikely.

Finally, the type of crystal found is consistent with long-range forces being operative. In protein crystals neighbouring molecules are in contact and this also seems to be true of the small crystallisable viruses. The particles of bushy stunt virus and turnip yellow mosaic virus[18,19], which, incidentally, also have icosahedral symmetry, crystallise in a body-centred cubic structure in which each particle is surrounded by[8] others in contact with it. In contrast, in the TIV crystal the particles are arranged in a close-packed configuration which fills space as uniformly as possible. This is what would be expected if the arrangement in the crystal were determined mainly by non-directional forces.

This does not, of course, mean that the virus particles would necessarily show random spherical rotational disorder, since the particles themselves are not spherical so that residual directional effects are quite possible. From our observations of the two lowest order Bragg reflections alone, it cannot be established whether such disorder exists or not. This question could best be settled either by an X-ray diffraction photograph of a single crystal or by one of a polycrystalline mass ("powder diagram") taken at sufficient resolution to show crystal reflections, but neither of these has been obtained because of the serious technical difficulties involved. Hence we cannot as yet conclude that the virus particles are in fixed orientations in the wet crystal, although this is certainly the case in the methacrylate-embedded microcrystals, as shown by WILLIAMS AND SMITH's electron micrographs[3].

The condition of equilibrium at a definite distance which may be varied very easily would follow if the equilibrium were determined by the interplay of *weak* attractive and repulsive forces operating through the water between the particles. On current views the attraction would be provided either by simple van der Waals forces, which have been demonstrated to exist between extended solids[26,27], or possibly by the KIRKWOOD-SHUMAKER[28,29] forces arising from the fluctuating proton distribuion in protein molecules. Whatever the exact mechanism, the point is that these are forces which act at distances of the same order as the size of the particles themselves[30–32,*].

* The crystalline bacterial arrays observed by GOLDACRE[33] ought perhaps to be referred to here as well, but the distances in this case are of the order of about ten times or more as great as those between colloidal (or virus) particles, and the forces are probably of quite a different kind.

References p. 219.

The repulsive forces originate in the ionic double layer which surrounds the particles and the thickness of which is inversely proportional to the square root of the salt concentration. That such forces act between particles of TIV in solution is shown by the fact that a small amount of added salt reduces the stability of the colloidal solution and causes the virus to precipitate. Finally, in order that a condition of equilibrium be possible, it is necessary that the thermal energy be less than the depth of potential minimum. For a particle as large as TIV, this requirement would probably be easily satisfied; in fact, VERWEY AND OVERBEEK[24] have shown by simple numerical arguments that, for particles of dimension greater than about 100 Å, Brownian motion has little effect on the stability of sols[32].

If the interpretation given above is correct, the ordering of the particles of TIV into a crystal lattice is of great interest for colloid physics. Hitherto ordering at interparticle distances larger than the particle diameter has been observed only for anisodimensional particles having the shape of either plates (*e.g.* ferric hydroxide[8,9]) or rods (tobacco mosaic virus[25]). By contrast, TIV seems to represent the first observed instance of the crystalline ordering of approximately spherical, and hence isometric, particles. In this case, however, the ordered phase is formed at a concentration ($\sim$ 17 %) much greater than that required in the case of the rod-shaped TMV (2.5 %[34]). This is to be expected if particle asymmetry facilitated the separation of an ordered phase[7,35].

Since TIV is obtainable in fairly large quantities and is readily purified, and moreover, since the virus particles, though large, are remarkably uniform, it seems that this virus may provide the ideal material for a quantitative study of the physical chemistry of a well-defined colloidal system consisting of isometric particles. It has the further advantage that changes in the interparticle distance can, as we have shown, be followed with visible light. It should, however, be emphasized that the implications for the theory of long-range forces of the work presented here can only be considered as tentative. Quantitative investigations of the effects of virus concentration, temperature and, above all, of salt concentration and pH on the crystal structure of TIV have yet to be made.

APPENDIX

SECOND-ORDER EFFECTS IN THE OPTICAL ANALYSIS

A. KLUG

Deviation from the Bragg Law

The non-linearity of the λ^2 *vs.* $\cos^2\alpha$ plots in Fig. 5 will now be considered. In view of the accuracy of the optical measurements a detailed investigation of this effect is justified, and is indeed necessary to establish the correctness of the general conclusions and of the numerical values obtained from the use of Bragg's law (equation (2)). The extent of the deviation from the simple Bragg law is best shown in Fig. 6, which shows a plot of λ against $\sin\theta$ for the 111 reflection, where θ has been calculated from α by using equation (1) and a value of 1.365 for n_e. The deviation from the straight line drawn through the points of lowest $\sin\theta$ is quite obvious, and well beyond experimental error. The relative discrepancy is only about 1 %, but it is the absolute value that is important. At values of $\sin\theta$ near unity, the discrepancy $\delta(\sin\theta)$ is

References p. 219.

about 0.008 ± 0.003, corresponding to a deviation in θ of 8°. If a different value of n_c is used (1.377) the magnitude of the discrepancy at high values of sin θ is reduced only a little.

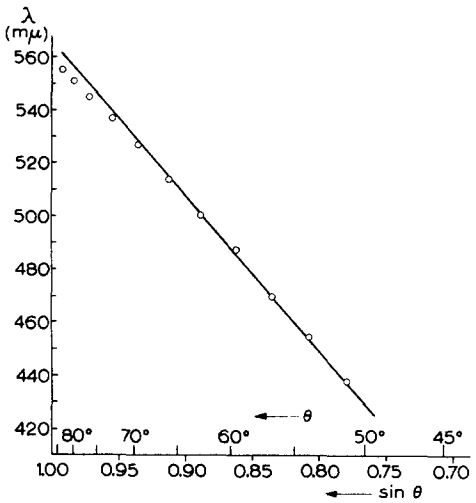

Fig. 6. The wavelength λ corresponding to maximum intensity of the 111 reflection plotted against sin θ, to show the deviations from the Bragg law (equation (2)).

Broadening of the reflections

As mentioned above, the effect described is related to the small thickness of the crystal under observation. It is difficult to measure the thickness directly, but a very rough estimate of the average thickness t may be made from the angular range over which the Bragg reflection is observed to take place. If β is the half-width in radians of the reflected Bragg peak, then the well-known Scherrer formula of X-ray crystallography gives

$$t = Nd = \lambda'/\beta \cos\theta \tag{4}$$

λ' refers to the wavelength in the crystal, *i.e.*, $\lambda' = \lambda/n_c$, so that using equation (1), the formula may be rewritten:

$$t = \lambda/\beta \cos\alpha \tag{4a}$$

A very rough visual estimate of β for the 111 reflection at high glancing angles gives about 5–8°, so that from equation (4), the average thickness of the crystals is calculated to be about 2–3 μ. This value can only be considered as giving an order of magnitude.

The shift in the position of maximum intensity

The intensity of light diffracted by a lattice[36] is a product of two functions: (a) the "lattice peak function", P, which has a maximum when the Bragg condition is satisfied, and (b) a scattering function, I, representing the light scattered by the individual particles of the lattice.

The breadth of the peak of the function P depends on how many crystal planes are cooperating, and its form as a function of sin θ, can be represented to a good approximation[36] by the Gaussian (see Fig. 7)

$$A \exp\left[-(x - x_0)^2/2\sigma^2\right],$$

References p. 219.

where $x = \sin\theta$, $x - x_0$ is the displacement of $\sin\theta$ from the value x_0 corresponding to the Bragg condition, and 2σ is approximately the half-width (in $\sin\theta$) of the peak. The latter is inversely proportional to the crystal thickness and from equation (4) it is given by

$$2\sigma = \lambda'/2t \tag{5}$$

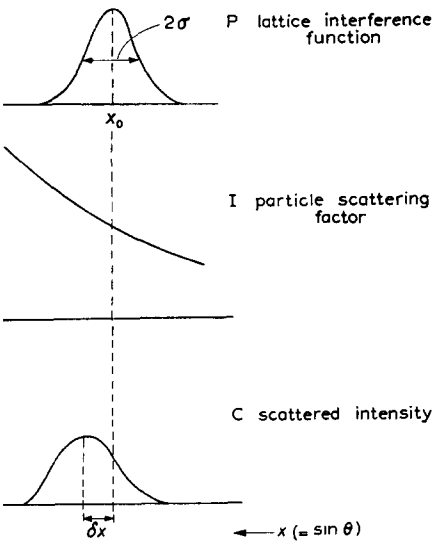

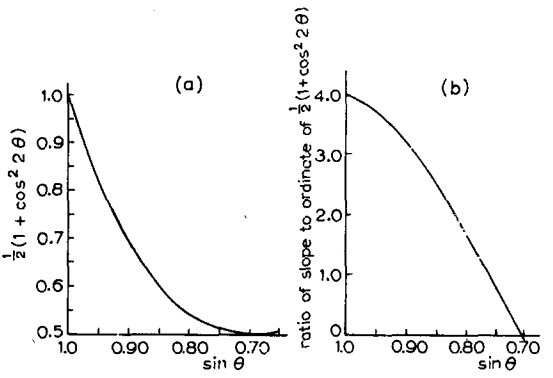

Fig. 8. (a) The polarisation factor $\frac{1}{2}(1 + \cos^2 2\theta)$, (b) the ratio between its slope and ordinate, as functions of $\sin\theta$.

Fig. 7. Scattering from crystals of small thickness. The scattered intensity (C) near a Bragg, reflection is the product of the lattice interference function (P) and the scattering power (I) of the asymmetric unit in the crystal. The shift in the position of the maximum, δx, is approximately equal to $\sigma^2 I'(x_0)/I(x_0)$

The form of the scattering function depends on the size, shape and refractive index of the individual particles. If they are points, I does not vary with θ (apart from a polarisation factor) and the effect of finite crystal size is simply to broaden the peak P as described above, the maximum in the product PI occurring at the value x_0 given by P alone. But if the particles have sizes approaching the wavelength of light, I is a function of $\sin\theta$, and the maximum of the product PI is displaced. The effect is illustrated in Fig. 7. If the ordinate and slope of I in the neighbourhood of x_0 are $a = I(x_0)$ and $m = I'(x_0)$ respectively, it is easy to show that, for $m\sigma/a \ll 1$, the shift in the position of the maximum is approximately given by

$$\delta x \equiv x - x_0 = \sigma^2 m/a \tag{6}$$

It is seen that the narrower the peak in P, *i.e.* the smaller σ, the less is the displacement. Thus if the crystals are not too thin, or alternatively if the scattering function is varying only slowly with angle, the effect can be ignored. (This is usually the situation in the case of X-ray diffraction by crystals). In the case of the TIV crystals, however, we, believe the displacement to be appreciable and we shall show that the non-linearity in Fig. 6 can be accounted for by the use of equation (6). Since, by equation (5), σ is independent of $\sin\theta$, the variation of the displacement from the straight line with $\sin\theta$ will be determined solely by the scattering function I.

In order to estimate the angular dependence of the intensity of light scattered by

References p. 219.

a virus particle, calculations have been made using the MIE[37,38] theory for a spherical particle of refractive index 1.5 immersed in water. The parameter $2\pi D/\lambda'$, where D is the diameter of the particle, was given various values in the range 1.6–2.0, corresponding to the range of the wavelengths used in the optical observations and to values of D ranging from 1300–1700 Å. The results were very little different from similar calculations made using the simpler Rayleigh-Gans theory, in which the difference in refractive index between the particle and the immersion medium is neglected. The latter theory is thus adequate for our purposes.

On the Rayleigh theory, the scattered intensity I for unpolarised* incident light is given by an expression of the form

$$I \propto \frac{1}{\lambda'^4} \psi (\sin \theta/\lambda') \{ 1 + \cos^2 2\theta \} \tag{7}$$

where ψ is a function depending on the size and shape of the particles. However, under the conditions of our observations, $\sin \theta/\lambda'$ is a constant or at least very nearly so (Bragg's law), so that ψ may also be taken as constant. Hence, irrespective of the particular shape and size of the virus particle in solution, the required angular dependence of the scattered intensity is effectively given by the polarisation factor (see Fig. 8a):

$$1 + \cos^2 2\theta = 1 + (1-2 \sin^2 \theta)^2 \tag{8}$$

It follows from equations (6) and (7) that the variation of the displacement in the position of the maximum intensity diffracted by the crystal is determined by the ratio between the slope and ordinate of the polarisation factor. This ratio is plotted as a function of $\sin \theta$ in Fig. 8b, and it will be seen that the extent of the deviation from the straight line in Fig. 6 varies in a manner similar to this curve.

From equations (6) and (8), the displacement at $\sin \theta = 1$ is equal to $4\sigma^2$. Estimating the deviation in $\sin \theta$ from the simple Bragg law to be 0.01 in the neighbourhood of $\sin \theta = 1$ (see Fig. 6), we thus have

$$\sigma^2 = 0.0025$$

from which $\sigma = 0.05$. Hence from equation (5), the average crystal thickness t is

$$t = \frac{3600}{4 \cdot 0.05} \text{ Å}$$
$$= 1.8 \mu$$

This corresponds to about $N = 7$ cooperating planes.

This estimate of the average crystal thickness is much more reliable than that obtained from attempting to judge visually the half-width, and moreover seems to correspond nicely to the width of 1.5 μ found for the smallest striations observed in the crystals. At all events, we may take the argument the other way. If a high proportion of the crystals or crystal domains are as thin as 1.5 μ, (as is quite frequently observed), then the Bragg law would not be obeyed exactly, and second order deviations of the magnitude actually observed are to be expected. We may, therefore, safely conclude that the optical phenomena may be described as rather broadened

* There will be a certain amount of depolarisation due to reflection at the surfaces of the perspex window, but a calculation[39] shows that, even at the Brewster angle, it is only about 15 %.

References p. 219.

Bragg reflections, and that the method described above for determining the unit cell dimensions is valid.

ACKNOWLEDGEMENTS

We wish to thank Professor R. C. WILLIAMS and Dr. K. M. SMITH for their interest and for supplying us with the virus preparations, and Mr. G. ATKINSON for the colour photography. This work was supported in part by the Agricultural Research Council (R.E.F.) and the Nuffield Foundation (A.K.), and in its later stages by a research grant, No. E-1772, from the Institutes of Health of the United States Public Health Service. Thanks are also due to the Council of the Royal Society for a grant from the Scientific Investigations Grant-in-aid (S.P.F.H.-O.).

REFERENCES

1 N. XEROS, *Nature*, 174 (1954) 562.
2 K. M. SMITH, *Nature*, 175 (1955) 12.
3 R. C. WILLIAMS AND K. M. SMITH, *Nature*, 179 (1957) 119.
4 K. M. SMITH AND R. C. WILLIAMS, *Endeavour*, 17 (1958) 12.
5 R. C. WILLIAMS AND K. M. SMITH, *Biochim. Biophys. Acta*, 28 (1958) 464.
6 M. H. F. WILKINS, A. R. STOKES, W. E. SEEDS AND G. OSTER, *Nature*, 166 (1950) 127.
7 G. OSTER, *J. Gen. Physiol.*, 33 (1950) 445.
8 H. ZOCHER AND K. JACOBSOHN, *Kolloid-Beih.*, 28 (1929) 167.
9 P. BERGMANN, P. LÖW-BEER AND H. ZOCHER, *Z. physik. Chem. (Leipzig)* A, 181 (1938) 301.
10 W. MENKE, *Z. Naturforsch.*, 12b (1957) 407.
11 T. ALFREY JR., E. B. BRADFORD, J. W. VANDERHOFF AND G. OSTER, *J. Appl. Phys.*, 44 (1954) 503.
12 C. ROBINSON, *Trans. Faraday. Soc.*, 52 (1956) 571.
13 LORD RAYLEIGH, *Phil. Mag.*, 26 (1888) 256.
14 G. E. PERLMANN AND L. G. LONGSWORTH, *J. Am. Chem. Soc.*, 70 (1948) 2719.
15 L. W. LABAW AND R. W. G. WYCKOFF, *Science*, 123 (1956) 849.
16 L. W. LABAW AND R. W. G. WYCKOFF, *Arch. Biochem. Biophys.*, 67 (1957) 225.
17 R. L. STEERE, *J. Biophys. Biochem. Cytol.*, 3 (1957) 45.
18 D. L. D. CASPAR, *Nature*, 177 (1956) 476.
19 A. KLUG, R. E. FRANKLIN AND J. T. FINCH, *Biochim. Biophys. Acta*, 25 (1957) 242.
20 B. E. MAGDOFF, private communication.
21 K. M. SMITH, *J. Biophys. Biochem. Cytol.*, 2 (1956) 301. K. M. SMITH, *Nature*, 181 (1958) 966.
22 M. A. LAUFFER, *Advances in Virus Research*, 2 (1954) 241.
23 U. W. ARNDT AND W. W. BEEMAN, private communication.
24 E. J. W. VERWEY AND J. T. OVERBEEK, *Theory of the Stability of Lyophobic Colloids*, Elsevier, Amsterdam, 1948.
25 J. D. BERNAL AND I. FANKUCHEN, *J. Gen. Physiol.*, 25 (1941) 111.
26 I. B. V. DERJAGUIN AND I. I. ABRICOSSOVA, *Discussions Faraday Soc.*, 18 (1954) 33.
27 J. A. KITCHENER AND A. P. PROSSER, *Proc. Roy. Soc. London A*, 242 (1957) 403.
28 J. G. KIRKWOOD AND J. B. SHUMAKER, *Proc. Nat. Acad. Sci. U.S.*, 38 (1952) 863.
29 J. G. KIRKWOOD, in *Symposium on Biocolloids, J. Cellular Comp. Physiol.*, 49, Supplement 1 (1957) 59.
30 J. D. BERNAL, *Trans. Faraday Soc.*, 42B (1946) 1, 130.
31 J. D. BERNAL, *Colloq. Intern. centre Natl. recherche sci.* (Paris), 53 (1953) 1, particularly page 11.
32 G. OSTER, in *Symposium on Biocolloids, J. Cellular Comp. Physiol.*, 49, Supplement 1 (1957) 129.
33 R. J. GOLDACRE, *Nature*, 174 (1954) 732.
34 F. C. BAWDEN AND N. W. PIRIE, *Proc. Roy. Soc. London B*, 123 (1937) 274.
35 L. ONSAGER, *Ann. N. Y. Acad. Sci.*, 51 (1949) 627.
36 R. W. JAMES, *The Optical Principles of the Diffraction of X-rays*, Bell, Edinburgh, 1948.
37 G. MIE, *Ann. Physik*, 25 (1908) 377.
38 G. OSTER, *Chem. Revs.*, 42 (1948) 319.
39 F. A. JENKINS AND H. E. WHITE, *Fundamentals of Optics*, 3rd ed., McGraw Hill, New York, 1957, Section 24.4.